

Stepanyuk, Sergey; Bruns, Rainer; Krivenkov, Konstantin

Article

Empirical lateral-force-model for forklift tires

Logistics Research

Provided in Cooperation with:

Bundesvereinigung Logistik (BVL) e.V., Bremen

Suggested Citation: Stepanyuk, Sergey; Bruns, Rainer; Krivenkov, Konstantin (2017) : Empirical lateral-force-model for forklift tires, Logistics Research, ISSN 1865-0368, Bundesvereinigung Logistik (BVL), Bremen, Vol. 10, Iss. 1, pp. 1-12, https://doi.org/10.23773/2017_1

This Version is available at:

<https://hdl.handle.net/10419/182046>

Standard-Nutzungsbedingungen:

Die Dokumente auf EconStor dürfen zu eigenen wissenschaftlichen Zwecken und zum Privatgebrauch gespeichert und kopiert werden.

Sie dürfen die Dokumente nicht für öffentliche oder kommerzielle Zwecke vervielfältigen, öffentlich ausstellen, öffentlich zugänglich machen, vertreiben oder anderweitig nutzen.

Sofern die Verfasser die Dokumente unter Open-Content-Lizenzen (insbesondere CC-Lizenzen) zur Verfügung gestellt haben sollten, gelten abweichend von diesen Nutzungsbedingungen die in der dort genannten Lizenz gewährten Nutzungsrechte.

Terms of use:

Documents in EconStor may be saved and copied for your personal and scholarly purposes.

You are not to copy documents for public or commercial purposes, to exhibit the documents publicly, to make them publicly available on the internet, or to distribute or otherwise use the documents in public.

If the documents have been made available under an Open Content Licence (especially Creative Commons Licences), you may exercise further usage rights as specified in the indicated licence.



<https://creativecommons.org/licenses/by/4.0/>

Empirical Lateral-Force-Model for Forklift Tires

Sergey Stepanyuk¹ | Rainer Bruns¹ | Konstantin Krivenkov¹

Received: 22 March 2016 / Accepted: 21 March 2017 / Published online: 19 September 2017
© The Author(s) 2017 This article is published with Open Access at www.bvl.de/lore

Abstract Operational safety is the major aspect of a counterbalanced forklift's design. A new test was introduced with the standard DIN EN 16203 to test the lateral dynamic safety of forklifts. The measurements involve high costs and effort to achieve reproducible results. Multibody simulations (MBS) are conducted to facilitate the design of safety systems and understand the safety limits of an industrial truck. An adequate tire model is an essential part of such simulation. A new approach to forklift tire modeling is presented in this paper. It involves measuring several common industrial tires on a drum tire testing apparatus and using them to parametrize the tire model. The SUPREM model (German: Superelastisches Reifenmodell) uses a mathematical modeling approach to describe lateral force and lateral tire deformation based on wheel load, slip angle, slip rate, and driving velocity. For this easy-to-use model, 8 parameters are estimated from tire measurements for different tire types. Better tire approximation leads to more accurate multibody simulations and a deeper understanding of the dynamic behavior of forklifts. Better vehicle lateral stability can be achieved if the outcomes are considered in the design process of a forklift. With this model highly dynamic multibody forklift simulations according to DIN EN 16203 can be carried out.

Keywords Tires · Modeling · Multibody Simulation · Lateral Force · Lateral Stability

✉ Sergey Stepanyuk
sergey.stepanyuk@hsu-hh.de

Rainer Bruns
rainer.bruns@hsu-hh.de

Konstantin Krivenkov
konstantin.krivenkov@hsu-hh.de

1 Necessity of the multibody simulation

The dynamic stability plays a crucial role in the operation of a forklift. It is determined by the geometrical dimensions, the tire characteristics and the position of the overall center of gravity. The tire performance determines whether a vehicle tilts or slides into a sharp turn. To improve the dynamic stability and prevent forklifts from tilting active systems such as Toyota's "SAS" and Jungheinrich's "Curve Control" are used. In order to ensure that a forklift truck is sufficiently safe to operate, it is very important to have exact knowledge of the dynamic properties of the tire.

Many attempts have been carried out to describe the dynamic stability quantitatively (see [4], [15] and [16]). The standard DIN ISO 22915-2 describes simple tests for measuring the static and dynamic stabilities on a tilting platform. The data on the behavior of a vehicle in a bend can be deduced from the lateral tilt angle. The standard DIN EN 16203 has been developed to reach a definite conclusion regarding forklift dynamic stability and to assess the influence of the active stability systems. The standard describes a course in which an L-shaped sharp turn is made at full speed. The necessary width of the exit corridor for this maneuver is used as the benchmark.

The conduct of an L-test poses many difficulties. A particular challenge is posed by the technical effort needed to achieve reproducible results. To reduce the experimental effort required for new forklift prototypes, multibody simulations in which dynamic stability is assessed are carried out. A tire model is needed for a multibody simulation to be meaningful. Many numerical tire models represent the behavior of pneumatic tires, for example, UA Tire Model [11] and Pacejka's "Magic Formula" [20]. Many models are commercially

¹ Professorship of Machine Elements and Technical Logistics
Helmut Schmidt Universität, Holstenhofweg 85,
22043 Hamburg, Germany

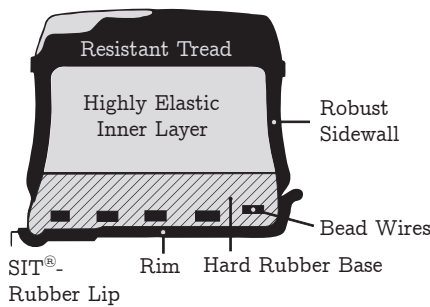


Fig. 1: Schematic structure of an SE-tire (Reference: Continental AG, Hanover)

available in simulation software. All the models can be subdivided into mathematical, semi-physical and physical models, according to the approach taken. Mathematical models use a phenomenological approach and determine the tire behavior by mathematical approximation equations. Such models for agricultural machinery are described in [23] and [17]. Mathematical models are easy to use, quick or real time capable and offer a high degree of precision. Effects like vibration and interaction with obstacles, however, cannot be described and more intensive measurements are needed to determine all the model parameters. Semi-physical or physical models are used to make better predictions for ground-tire-interaction. It is often not easy to make strict distinctions. Some models use a mathematical approach for the tire combined with a physical approach in the contact area as in MF-Swift tire model [1]. Semi-physical models like [18] and [24] are built of strings or brushes and can predict pressure distribution in the ground. A further improvement can be achieved by using one or more interacting rigid or flexible belt elements to describe the carcass of the tire. Such models can be used to describe comfort and vibration transmission in the tire (see CTire [12], FTire [13] and CDTire [10]). The approach that is most time consuming, but at the same time provides the most insight involves the use of the 3-dimensional FEM (finite element method) analysis as in [2] and [3].

Super elastic tires (SE-tires) have their origin in pneumatic tires that are filled with soft rubber [21]. Fig. 1 shows a schematic representation of a tire-rim combination. The tire can be made of several asymmetrical layers of rubber. Every rubber layer is specially designed to ensure low abrasion; low vibration transfer or uniform heat distribution. Standard models, however, are primarily designed for tires filled with air used in automotive applications. They are only partially applicable to super elastic forklift tires. This can be explained by different operational conditions such

as low speed combined with increased maneuverability (high slip angles) and construction differences.

To obtain more understanding about forklift behavior tires were measured under various operating conditions. From the measurement data, an empirical tire model for static and dynamic behavior was developed. Model parameters for 5 different tire types were estimated to be used in further multibody simulations.

2 Measuring forklift tires

To determine the behavior of tires used in later multibody simulations, the tire testing apparatus that had been built for previous projects at the Professorship of Machine Elements and Technical Logistics was used (see Fig. 2). The tire testing apparatus was specifically designed to measure a wide range of super elastic forklift tires. Sensors in the measurement platform allow to obtain 3 forces and 3 torques along each axis in addition to traveling speed and slip angle. The coordinate system used in the apparatus is depicted in Fig. 3. The following parameters can be set:

- Speed: 0 ... 25 km/h
- Slip angle: $-90^\circ \dots +90^\circ$
- Slip angle change rate: 0 ... 90 $^\circ$ /s
- Wheel load: 0 ... 35 kN
- Tire diameter: 80 ... 850 mm

A measurement program that allows a wide variety of operating conditions to be measured was developed. The variation of the slip angle and the wheel load is particularly interesting for determining the lateral behavior of a tire. The slip angle α is the angle between the intersection line of wheel plane and road plane and the vertical projection of the tire trajectory velocity vector on the road plane [9]; the slip rate $\dot{\alpha}$ is thus the time derivative of the slip angle. The wheel load was increased up to the nominal load in 3 steps during the tire measurement. In each step, the slip angle was adjusted within a range of -45° to $+45^\circ$ while the speed and slip rate were also gradually increased. Due to a short measurement time, the temperature increase in a tire is low. The thesis by Busch [5] showed a small influence of temperature on the lateral force. In order to keep the influence of the momentum of the test apparatus as low as possible and emphasize the dynamic effects in the tire, all the measurements were carried out at slip rates of between 15 $^\circ$ /s and 30 $^\circ$ /s and a speed of between 0.5 km/h and 25 km/h.

The measured data includes noise in a relatively broad frequency range, which can be attributed to sev-



Fig. 2: Tire testing apparatus at the Professorship of Machine Elements and Technical Logistics

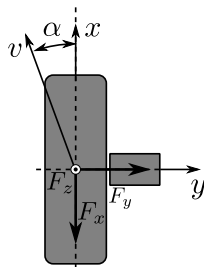


Fig. 3: Tire coordinate system

eral causes. The tread pattern yields a fluctuating load force profile in the medium-frequency range. The tire testing drum has a 2-component polyurethane coating with quartz sand embedded (grain diameter 0,4-0,7 mm) to reproduce the tarmac friction characteristic. This coating leads to high-frequency noise. Small deviations in the centering of the tire that arise during assembly and the irregularity of the tire material cause severe low, tire-rotation-periodic oscillations. These are especially noticeable at low speeds. These parasitic side effects can be almost eliminated by suitably filtering the measured data. For visualization purposes a 2nd order Bessel filter with a limit frequency of 1 Hz with phase

shifting elimination was used. Raw data was used to estimate the model parameters.

3 Static tire model

3.1 Model requirements

The thesis by Busch [5] provides a comprehensive insight into the lateral dynamic behavior of super elastic tires. In this study, a model using artificial neural networks has been built. This model provides physically correct values, but has disadvantages typical of neural networks.

The creation of training data is in itself a complicated task and inopportunately selected data can lead to an over-adaptation of the network. It is compounded by the fact that the use of artificial neural networks allows only limited insight to be gained into the actual physics of the tire. In addition, several weighting matrices describe the network, which is cumbersome in practice. And finally, the insufficient extrapolating ability of the neural network can lead to wrong predictions outside of the boundaries of training data set. This can cause problems when sharp cornering is modeled because the wheel load often exceeds the rated load of the tire.

For these reasons, an empirical approach was adopted for the Super Elastic Tire Model (SUPREM). The SUPREM allows a high approximation quality to be achieved with a minimum of tests. At the same time, the model allows a deeper insight to be gained into the behavior of the tire. Unlike a theoretical model (for example involving the use of an FEM calculation) the amount of computational work required should stay low.

The following objectives were pursued during the creation of the model:

- The model must be valid for different types of SE-tires without the model structure being changed.
- The model should be easy to implement.
- The number of input variables and parameters should be kept low.
- The model should be applicable to other types of tires.
- The effort required to parametrize the model using the measured data should be low.

3.2 Static behavior of tires

Fig. 5 shows the typical lateral force behavior of an SE-tire. The main factors are the slip angle α and the wheel load F_Z which both have an impact on the lateral force. The lateral force increases with higher wheel load, while with higher slip angle the lateral force converges towards a constant value.

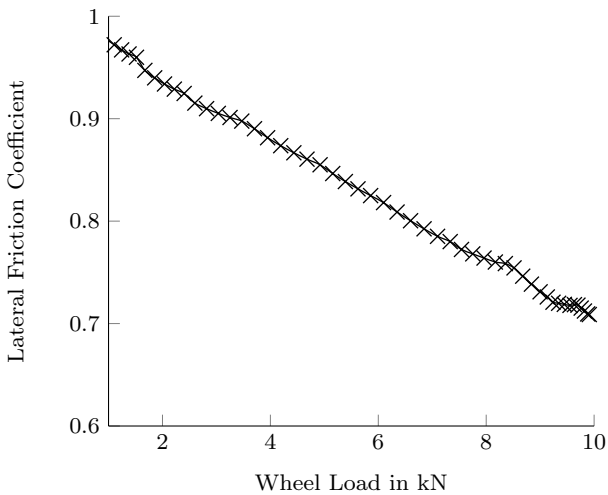


Fig. 4: Quasi-static lateral friction coefficient (Reference: [5]) (Tire: 18x7-8; $\alpha = 45^\circ$; $v = 12$ km/h); rated load capacity 16180 N

If the slip rate is low, no hysteresis should form and the graph passes through the graph origin. This be-

havior can be described as stationary and be approximated by a hyperbolic tangent function. It is origin-symmetrical and runs for rising angles to +1 or -1. The argument of the hyperbolic tangent function describes the slope of the curve at the graph origin and hence the "speed" at which the function reaches its final value.

The function argument is affected by the slip angle and the wheel load. Larger slip angles lead to a higher lateral force that converges for high slip angle values. A higher wheel load causes higher maximum lateral forces, but reduces the influence of the slip angle on the overall lateral force. When the load on the wheels is higher, the stiffness of the materials used in such wheels increases, resulting in higher rotational stiffness. Increasing rotational stiffness leads to a deterioration in lateral force transmission at small slip angles. These observations lead to the following approach for describing the lateral force:

$$F_{Y,\text{stat}} = F_Z \cdot \mu \cdot \tanh\left(\frac{\alpha}{k_\alpha + k_{F2} \cdot F_Z}\right). \quad (1)$$

F_Z is the wheel load, μ is the coefficient of lateral friction and k_α and k_{F2} are parameters available for the approximation of the model to the measured data. Parameters k_α and k_{F2} define load-independent and load-dependent parts of the normalization term and adjust the influence of the slip angle on the lateral force.

Fig. 4 shows the quasi-static lateral friction coefficient that was determined by measurement. The slip angle α is set at 45° . At this setup the maximum lateral force can be achieved. The wheel load was adjusted in 300 N steps up to 10 kN. Higher wheel loads could not be measured due to high heat development in the tire. When the loads are low, lateral friction coefficient shows a nearly linear dependence. When the loads are higher, especially when they are above the rated load of the tire (rated wheel load of 18x7-8 tire is 16180 N), the linear approximation leads to incorrect results being obtained because the modeled friction tends to zero and can also become negative. This happens under forklift truck safety test conditions where the wheel load can exceed twice the rated wheel load.

In further examinations, it was also determined that the lateral friction has a wheel load under proportional behavior. An approximation of the measured data by an exponential function with an estimated parameter k_{F1} leads to more accurate results being obtained. These observations lead to the following approach for describing the quasi-static friction coefficient:

$$\mu = \mu_B \cdot \exp\left(-\frac{F_Z}{k_{F1}}\right). \quad (2)$$

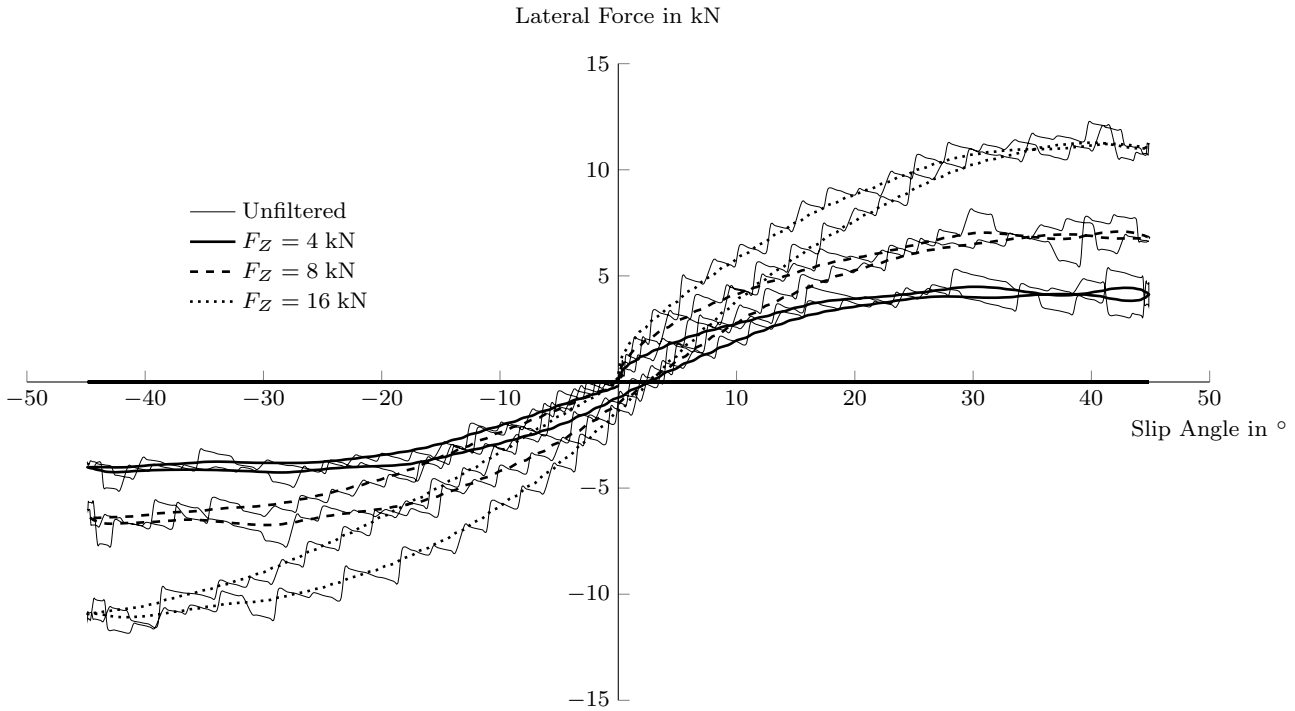


Fig. 5: Lateral force of an SE-tire (Tire: 18x7-8; $v = 12$ km/h; $\dot{\alpha} = 25$ °/s)

A standardized floor coating is used in the tire test apparatus. If a ride on another surface is to be simulated, the coefficient of friction μ_B must be set accordingly. With this addition, the model can be interpreted as follows:

$$F_{Y,\text{stat}} = F_Z \cdot \mu_B \cdot \exp\left(-\frac{F_Z}{k_{F1}}\right) \cdot \tanh\left(\frac{\alpha}{k_{\alpha} + k_{F2} \cdot F_Z}\right) \quad (3)$$

4 Dynamic tire model

Damping effects arise during a dynamic force change in a wheel. They appear in the measured data as a hysteresis, which is approximately symmetrical to the graph origin and is affected by the speed of the wheel and the temporary change of the lateral force. Such behavior can be explained theoretically using the string model (String-Type Tire Model) [19]. The tire contact patch is described as an interconnection of several pre-stressed strings connected to tread elements and having a certain stiffness. The deformation that takes place due to the load defines the transmission of lateral force. During a dynamic force change the transmission characteristics of the string model can be approximated by a PT_1 transfer behavior. In [22], examinations were car-

ried out on tractor tires and the results were found to be consistent with PT_1 transfer function behavior.

The entire tire model can be represented as a series connection of a static non-linearity and a linear transmission function. Models like these are called Hammerstein models and are a simplification of the Volterra series [14]. The general equation for the dynamic model can thus be formulated as follows:

$$F_{Y,\text{dyn}} + T \cdot \dot{F}_{Y,\text{dyn}} = F_{Y,\text{stat}}, \quad (4)$$

where T is the time constant.

Several measurements at different slip rates ($\dot{\alpha} = 5 \dots 90$ °/s) and speeds ($v = 0.5 \dots 25$ km/h) were carried out to verify the assumptions and determine the time constant. As a benchmark, the value of the hysteresis was selected when $\alpha = 0^\circ$, because at this point the change of the lateral force is at its maximum and the slip rate is constant. This leads to the maximal value of the hysteresis. Test results can be seen in Figs. 6 and 7.

When the slip rate rises, the width of the hysteresis increases. Increasing velocity at constant slip rate results in a narrower hysteresis. The linear relationship with the slip rate confirmed a proportional transmission characteristic with a delay of the first order. The time constant T , however, is only constant for a given vehicle speed v . A detailed study at constant wheel load, constant slip rate and variable speeds (see Fig. 7) showed

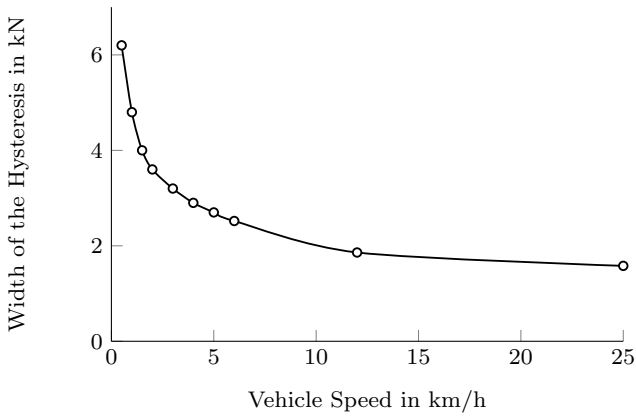


Fig. 6: Measured width of the hysteresis at $\alpha = 0^\circ$ as a function of the vehicle speed (Tire: 18x7-8; $F_Z = 4$ kN; $\dot{\alpha} = 25^\circ/\text{s}$)

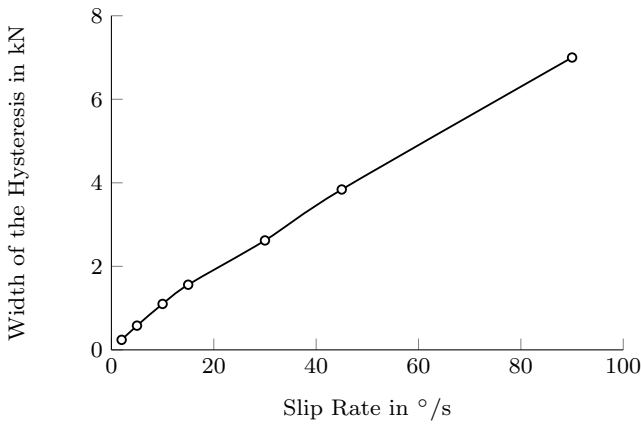


Fig. 7: Measured width of the hysteresis at $\alpha = 0^\circ$ as a function of the slip rate (Tire: 18x7-8; $F_Z = 8$ kN; $v = 15$ km/h)

that the time constant can be described by the following equation:

$$T = k_d \cdot (v \cdot 1 \text{ h/km})^{-k_v} . \quad (5)$$

The parameters k_d and k_v are estimated from measured data. The parameter k_v expresses the velocity dependence of the time constant. For just one measured velocity this parameter is set to 0, and only the constant part k_d is taken into account. A borderline case of this function occurs at a very slow speed ($v \rightarrow 0$). In that case, the equation 5 leads to a singularity. In the measurement at low velocities very high values of T could be calculated. This case is a limitation of the model. In the multibody simulation of the forklift, the tire model is only switched on after a short straight acceleration phase up to a velocity above 0,05 m/s.

The dynamic tire model leads to a more complex calculation process in the multibody simulation and

could result in instability during a numerical calculation. Especially the need for differentiation may cause a simulation to fail due to the occurrence of singularities. This can be prevented in many cases by adjusting the iteration step width. The static model provides good stability and accuracy but only by small temporary changes in the lateral force.

An L-test with a complete MBS model was carried out to estimate the magnitude of the slip rate. Rapid counter steering results in slip rates of more than $50^\circ/\text{s}$. As shown by a PT_1 transfer behavior, the shear force comes only with a delay, which makes extended steering phases necessary. It can therefore be concluded that only the dynamic tire model should be used to realistically assess the dynamic stability.

5 Deformation of the tire

When lateral stress develops, a deformation arises and leads to a displacement of the contact patch (see Fig. 8). This displacement of the outer wheels increases the tendency of a counterbalanced truck to tilt laterally. This effect can be described in the multibody simulation either by a displacement of the contact patch or by a tilting torque. The torque method was used to simplify the implementation. The torque is a product of the wheel load and the displacement in the y-direction (see Fig. 8). The torque is heavily dependent on the lateral force and is approximated linearly in the model:

$$M_X = F_Z \cdot \Delta y \approx \frac{F_Y}{k_M} . \quad (6)$$

The parameter k_M is estimated from measured data and describes this correlation. The torque is set at zero for the inner wheels. Although the contact patch is moved, the tilt edge of the vehicle as a whole is not affected.

6 Influences of rim geometry

The model described has symmetrical lateral force properties. According to measurements, that is not always the case. The differences in the deformation of the tire, which are dependent on the direction of the slip, could be clearly observed during the measurements. The inner flange of the rim supports the tire when lateral stress develops and reduces the deformation. As can be deduced from Fig. 8, significant deformation of the tire can reduce the contact patch and reduce transmittable forces. This behavior has also been observed in the measurement data. The parameter k_r is therefore inserted.

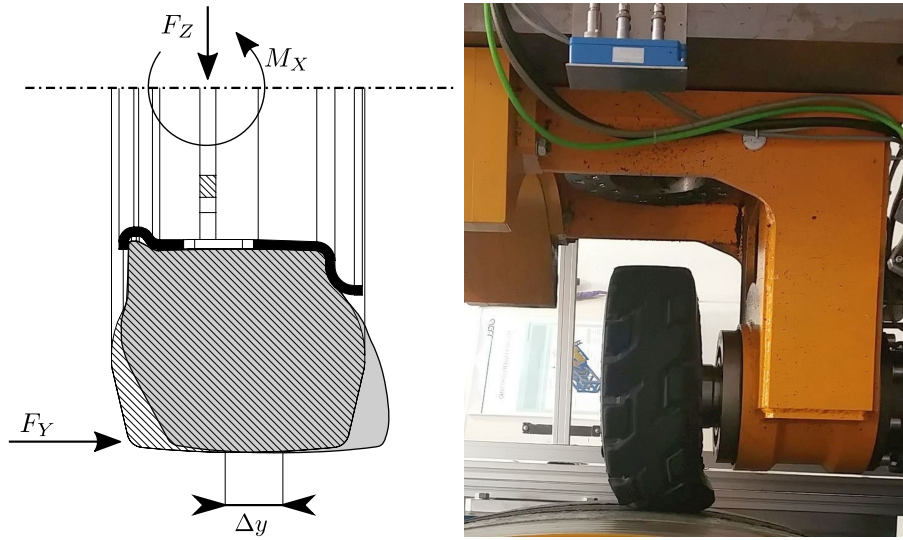


Fig. 8: Tire deformation under lateral force (tire type: 18x7-8)

It maps the dependence of the force on direction:

$$k_r(F_{Y,dyn}) = \begin{cases} 1 & \text{for } F_{Y,dyn} < 0 \\ k_r & \text{for } F_{Y,dyn} \geq 0 \end{cases} \quad (7)$$

This factor differs greatly from 1 only in some types of tires and is a product of distinct asymmetry of the rim and the internal tire structure. Thus, the model is extended by an additional nonlinearity of the linear transfer function. The following function describes the lateral force in an SE-tire:

$$F_Y = k_r(F_{Y,dyn}) \cdot F_{Y,dyn} \quad (8)$$

and therefore:

$$k_r \left(T \cdot \dot{F}_{Y,dyn} + F_{Y,dyn} \right) = F_Z \cdot \mu_B \cdot \exp \left(-\frac{F_Z}{k_{F1}} \right) \cdot \tanh \left(\frac{\alpha}{k_\alpha + k_{F2} \cdot F_Z} \right) \quad (9)$$

For time discrete systems with a step size of Δt it leads to following equations:

$$F_{Y,dyn_n} = \frac{1}{\frac{T}{\Delta t} + 1} \left[\frac{1}{k_r} F_{Y,dyn_n} + \frac{T}{\Delta t} F_{Y,dyn_{n-1}} \right], \quad (10)$$

$$F_{Y,dyn_n} = \frac{1}{\frac{T}{\Delta t} + 1} \left[\frac{1}{k_r} F_{Z,n} \cdot \mu_B \cdot \exp \left(-\frac{F_{Z,n}}{k_{F1}} \right) \cdot \tanh \left(\frac{\alpha_n}{k_\alpha + k_{F2} \cdot F_{Z,n}} \right) + \frac{T}{\Delta t} F_{Y,dyn_{n-1}} \right]. \quad (11)$$

7 Estimation of tire parameters

An optimization algorithm determines all six parameters of the model simultaneously from raw data. For every time step in the measurement file the tire model is evaluated. Deviations between model and measurement of every time step are used to calculate the Mean Square Error (MSE) which is used as an optimization function. The optimization is achieved with the Generalized Reduced Gradient (GRG), wherein the starting solution must be guessed. The solver minimizes this function to achieve its minimum. At the end of the optimization the model parameters are obtained at once. Numeric optimization does not always lead to a global minimum of the function and can stuck in one of local minima. A good guess of the starting solution (model parameters) can reduce calculation time needed. Although prior smoothing or filtering reduces the value of the optimization function, the impact on the estimated parameters is negligible. A comparison of the measurement and simulation results can be seen in Fig. 9.

The extrapolation ability of the model was also examined. The model was not configured with the complete data set, but only up to a wheel load corresponding to half the rated load. The subsequent extrapolation showed a deviation of less than 10 % in the lateral force. This ensures that even when short extreme loads are applied in dynamic simulations, extrapolation accuracy is sufficient. In order to assess the quality of the tire model, it was necessary to define a quality measure that corresponded to the coefficient of determination and was above 99 % for the model described so that the model has a high accuracy. The model therefore is suitable for simulative forklift stability tests.

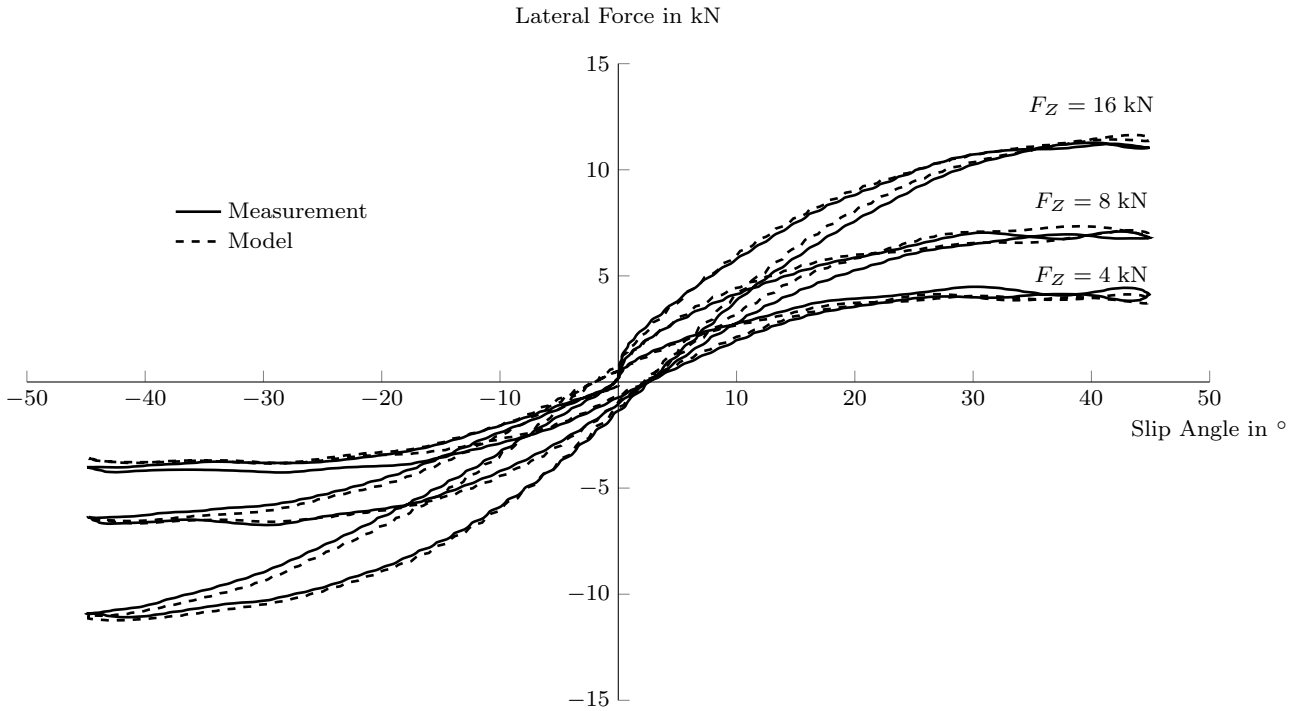


Fig. 9: Comparison of the simulation results and the measured data (Tire: 18x7-8; $v = 12$ km/h; $\dot{\alpha} = 25$ °/s; simulation at constant slip rate, measurement starts and stops at $\alpha = 0^\circ$)

8 Tire parameters

The lateral behavior of five tire types was measured. Three tires (200/50-10, 150/75-8 and 18x7-8) were examined according to their dynamic properties at different speeds. The dynamic time constant of some tires that were measured earlier and recycled could only be estimated for a velocity of $v = 12$ km/h. Parameters of the static model could be estimated in all cases.

Variations in the inner structure of the tires of different manufacturers, tire designs as well as fluctuations in the temperature and rubber mixture during the production can lead to fluctuations of the estimated parameters. One tire came from a different manufacturer and resulted in a very different lateral behavior (see tire 18x7-8 Manufacturer 2 in Table 2). Apparently, this tire was made out of a flexible rubber mixture. Curve fitting algorithms can also lead to fluctuations of calculated parameters. Model parameters presented in this paper may have their validity for a specific tire model of a specific manufacturer and give a rough correlation between geometrical dimensions and estimated parameters. A specific tire type of a given manufacturer used in a multibody simulation should be measured. A greater sample size is needed to account for different tire models of the same type and make a rough prediction of the tire behavior possible.

A wide range of tires was selected for the measurement in order to take account of different outer diameters, rims, load capacities and widths. Tire types 5.00-8, 18x7-8 and 200/50-10 have nearly the same outer diameter, but different widths. This helps to estimate the influence of the tire geometry on the lateral behavior. Dimensions of measured tires are summarized in Table 1 and estimated parameters in Table 2.

The rubber layer of the tire transfers forces from the vehicle to the road. The deformation capability of this layer influences the tire behavior. To compare different tires a cross-section-coefficient was defined as:

$$CSC = \frac{D_{out} - D_{in}}{2 \cdot W} \quad (12)$$

It takes the width W and the height of the rubber bondage into account (half of the difference between the tire diameter D_{out} and rim diameter D_{in}).

The parameter k_{F1} describes the amount of lateral force that can be transferred when a tire has a given load. Thin and high tires with higher cross-section-coefficients permit greater deformation and can transfer merely lighter forces to the road. According to the measurement, a thin 5.00-8 tire can transfer nearly 50 % of the force compared to a wider 200/50-10 tire when they have a given load. As shown in Fig. 11a, tires with comparable cross-section-coefficients tend to have a similar k_{F1} value.

	Unit	15x4.5-8	5.00-8	18x7-8	150/75-8 16x6-8	200/50-10
Type of rim		3.00 D-8		4.33 R-8		6.50 F-10
Width	mm	110	126	176	156	196
Diameter	mm	376	459	454	417	452
Rim diameter	mm	203	203	203	203	254
Tire height	mm	86.5	128	125.5	107	99
Cross-section coefficient	-	0.79	1.02	0.71	0.69	0.51
Load capacity (steer wheel)	kg	800	1090	1650	1150	1900
Load capacity (load wheel)	kg	1040	1415	2145	1455	2470

Table 1: Dimensions and load capacity of industrial tires (DIN 7811-1 [6], DIN 7811-2 [7], DIN 7852 [8])

The reaction of a tire to a slip angle is described by the parameter k_α . A tire type with higher cross-section-coefficients can be deformed more easily along the z-axis and therefore transfer less lateral force at a given slip angle. Higher values of the parameter k_α lead to a smaller argument of the hyperbolic tangent function and therefore lower lateral force at the given slip angle. Weaker influence of the slip angle (higher values for k_α) in tires with high cross-section-coefficient can be seen in Fig. 11b. The value of this parameter for wide tires is between 8° and 10° .

The two parameters k_α and k_{F2} are used to normalize the slip angle inside the hyperbolic tangent function. k_α normalizes the value of the slip angle by a specific angle. k_{F2} takes the stiffening effects of the tire load into account. The maximal load capacity was chosen as the reference load for estimating the normalization contribution of this term. Measurements show a correlation between the normalization terms (see Fig. 10).

Direction-dependent parameter k_r has a value of approximately 1 for wide tires and is slightly higher for tires with high cross-section-coefficient (see Fig. 12a).

The displacement of the contact area and therefore torque along the x-axis is described by the linearized parameter k_M . This parameter has a strong correlation with the cross-section-coefficient (see Fig. 12b). A flat and wide tire is less flexible and therefore better for dynamic vehicle stability.

k_v and k_d were able to be estimated for dynamic model parameters. The time constant T at a speed of $v = 12$ km/h was estimated for all the tires. As the cross-section-coefficient lowers, the value of the time constant diminishes until it reaches a value near 0.11 s.

Measurements for more different tires are needed to make rough predictions about an unknown tire. No measurements and therefore no assumptions were able

to be made for tires with load capacity above 3,5 t due to limitations in the measurement apparatus.

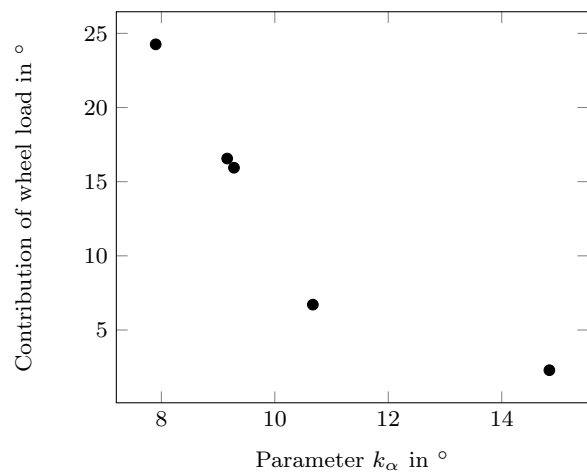


Fig. 10: Load-dependent-term ($k_{F2} \cdot F_{Z,nominal}$) as a function of the parameter k_α in the normalization term

9 Summary

In this paper, a SUPREM model has been set up for simulating SE-tires. It describes the transverse dynamic behavior with high accuracy. The original model, based on artificial neural networks, can be replaced by the SUPREM model without any loss of quality in approximation, but with significantly less complexity and with a potential for further adaptation. SUPREM model showed a better approximation quality especially for very high and very low lateral forces due to neural networks limitations. In the SUPREM model, a tire is described by six parameters only. By virtue of its

Parameter	Unit	15x4.5-8	5.00-8	18x7-8 Manufacturer 2	18x7-8 Manufacturer 1	150/75-8 16x6-8	200/50-10
k_{F1}	N	31451	25363	30522	50917	49241	55168
k_{α}	°	10.67	14.84	16.92	9.16	7.90	9.28
k_r	-	1.015	1.095	1.16	1.007	1.024	1.007
k_{F2}	°/N	$6.58 \cdot 10^{-4}$	$1.65 \cdot 10^{-3}$	$3.44 \cdot 10^{-4}$	$7.87 \cdot 10^{-4}$	$1.70 \cdot 10^{-3}$	$6.58 \cdot 10^{-4}$
k_M	-	13.45	22.09	14.84	11.91	11.79	12.90
k_v	-	-	-	-	0.39	0.43	0.20
k_d	s	-	-	-	0.28	0.31	0.19
$T_{v=12 \text{ km/h}}$	s	0.13	0.22	0.22	0.11	0.11	0.12

Table 2: Estimated tire parameters

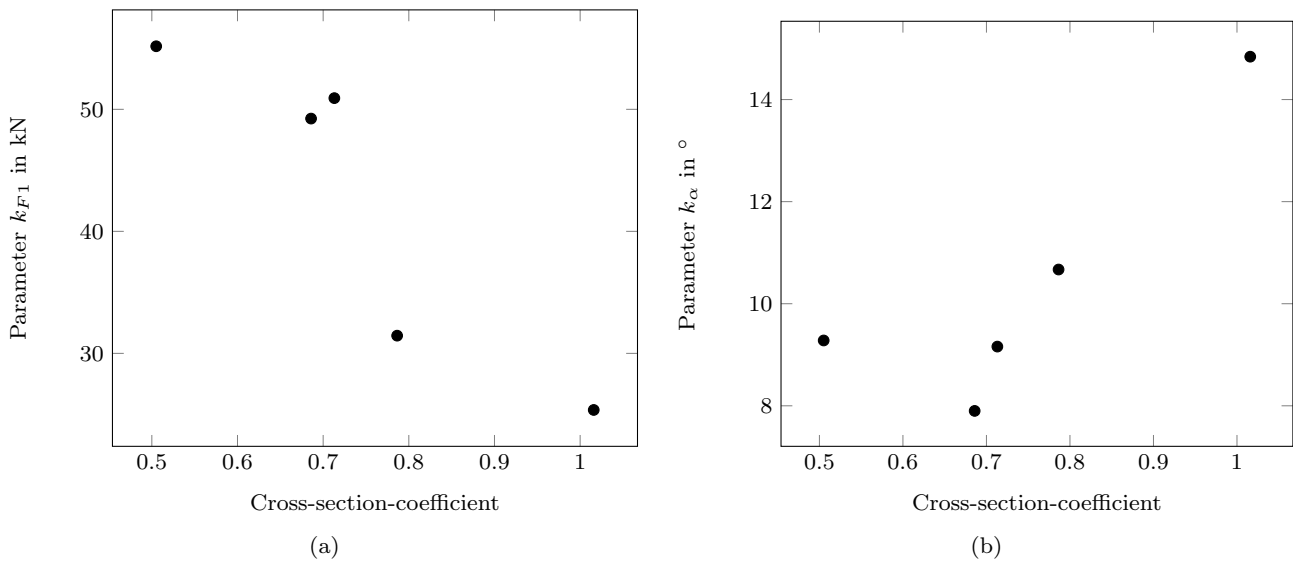


Fig. 11: (a) Parameter k_{F1} (b) Parameter k_{α}

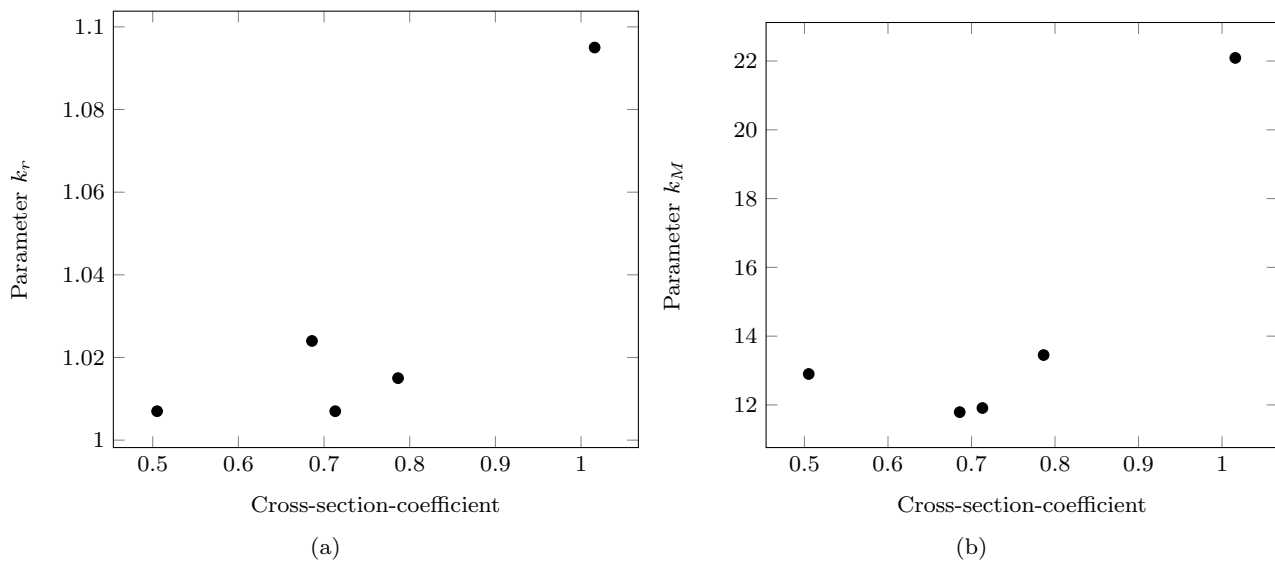
clear structure, the model can be easily integrated into many kinds of multibody simulation software without the need for costly additional modules.

When several comparable studies were conducted with the filtered and unfiltered data, it was found that the noise had a low impact on the estimated parameters.

Further studies have shown that the dynamic behavior is affected by high slip rates and must be taken into account during stability simulations. Multiple individual measurements must be carried out at different speeds to parametrize the hysteresis. The correlation of the slip rate with the width of the hysteresis requires only one parameter, so that only one measurement is necessary. Only one measurement is necessary if a vehicle is examined in a simulation in which approximately constant speeds are used.

Further studies must be conducted to ascertain whether the model is applicable to other types of tires such as portal stacker tires or polymer rollers. The influence of rubber and inner layer design used by differ-

ent manufacturers should be quantified. To validate the multibody simulation with this tire model additional empirical investigations with a forklift should be carried out.


 Fig. 12: (a) Parameter k_r (b) Parameter k_M

References

- Besselink, I., Pacejka, H., Schmeitz, A., Jansen, S.: The mf-swift tyre model: extending the magic formula with rigid ring dynamics and an enveloping model. *JSAE review* **26**(2) (2005)
- Biermann, J., von Estorff, O., Petersen, S., Schmidt, H.: Computational model to investigate the sound radiation from rolling tires 5. *Tire science and technology* **35**(3), 209–225 (2007)
- Brinkmeier, M., Nackenhorst, U., Volk, H.: A finite element approach to the transient dynamics of rolling tires with emphasis on rolling noise simulation 4. *Tire Science and Technology* (35), 165–182 (2007)
- Bruns, R., Busch, N., Höppner, O.: Anschlussbericht: Entwicklung eines dynamischen Standsicherheitstest für Gegengewichtstapler unter 10 t Tragkraft. Abschlussbericht (2009)
- Busch, N.: Querdynamisches Verhalten von Industriereifen und dessen Einfluss auf die Fahrdynamik von Gabelstaplern, *Berichte aus dem Institut für Konstruktions- und Fertigungstechnik*, vol. 40, 1. Aufl. edn. Shaker, Herzogenrath (2015)
- DIN 7811-1: Tyres for industrial and lift trucks; part 1: normal section sizes in diagonal construction. DIN Deutsches Institut für Normung e. V. (1994)
- DIN 7811-2: Tyres for industrial and lift trucks; part 2: wide section sizes in diagonal construction. DIN Deutsches Institut für Normung e. V. (1994)
- DIN 7852: Rubber solid tyres for pneumatic tyre rims. DIN Deutsches Institut für Normung e. V. (1994)
- DIN ISO 8855: Road vehicles - Vehicle dynamics and road-holding ability - Vocabulary. DIN Deutsches Institut für Normung e. V. (2013)
- Gallrein, A., Bäcker, M.: CDTire: a tire model for comfort and durability applications. *Vehicle System Dynamics* **45**(sup1), 69–77 (2007). DOI 10.1080/00423110801931771. URL <http://dx.doi.org/10.1080/00423110801931771>
- Gim, G., Nikravesh, P.E.: Comprehensive three dimensional models for vehicle dynamic simulations (1991)
- Gipser, M.: Reifenmodelle in der Fahrzeugdynamik: eine einfache Formel genügt nicht mehr, auch wenn sie magisch ist. Tagungsband, MKS-Simulation in der Automobilindustrie, Graz (2001)
- Gipser, M.: FTire—the tire simulation model for all applications related to vehicle dynamics. *Vehicle System Dynamics* **45**(S1), 139–151 (2007)
- Isermann, R.: Identifikation dynamischer Systeme. Springer-Lehrbuch. Springer, Berlin and Heidelberg [u.a.] (1988)
- Jérôme Rebelle, Pierre Mistrot, Richard Poirot: Development and validation of a numerical model for predicting forklift truck tip-over. *Vehicle System Dynamics* **47**(7), 771–804 (2009). DOI 10.1080/00423110802381216. URL <http://dx.doi.org/10.1080/00423110802381216>
- Lemerle, P., Höppner, O., Rebelle, J.: Dynamic stability of forklift trucks in cornering situations: Parametrical analysis using a driving simulator. *Vehicle System Dynamics* **49**(8/12), 1673–1693 (2011)
- Lines, J., Young, N.: A machine for measuring the suspension characteristics of agricultural tyres. *Journal of Terramechanics* **26**(34), 201 – 210 (1989). DOI [http://dx.doi.org/10.1016/0022-4898\(89\)90036-0](http://dx.doi.org/10.1016/0022-4898(89)90036-0)
- MASTINU, G., GAIAZZI, S., MONTANARO, F., PIROLA, D.: A semi-analytical tyre model for steady- and transient-state simulations. *Vehicle System Dynamics* **27**(sup001), 2–21 (1997). DOI 10.1080/00423119708969641. URL <http://dx.doi.org/10.1080/00423119708969641>
- Pacejka, H.B.: Analysis of the dynamic response of a rolling string-type tire model to lateral wheel-plane vibrations. *Vehicle System Dynamics* **1**, 37–66 (1972)
- Pacejka, H.B., Bakker, E.: The magic formula tyre model. *Vehicle System Dynamics* **21**(sup001), 1–18 (1992). DOI 10.1080/00423119208969994. URL <http://dx.doi.org/10.1080/00423119208969994>
- Rödiger, W.: Dr. Rödigers Enzyklopädie der Flurförderzeuge. AGT-Verl. Thum and Europa-Fachpresse-Verl, Ludwigsburg and München (2002)
- Schlotter, V.: Einfluss dynamischer Radlastschwankungen und Schräglaufwinkeländerungen auf die horizontale

- Kraftübertragung von Ackerschlepperreifen, *Forschungsbericht Agrartechnik des Arbeitskreises Forschung und Lehre der MEG*, vol. 437. Shaker, Aachen (2006)
23. Sharon, I.: Untersuchungen über die Schwingungseigenschaften großvolumiger Niederdruckreifen. (Forschungsbericht Agrartechnik des Arbeitskreises Forschung und Lehre der MEG [Max-Eyth-Gesellschaft]. Berlin (1975). Berlin, TU, Fachbereich Konstruktion u. Fertigung, Diss. v. 21.2.1975
24. Wang, Y.: Ein Simulationsmodell zum dynamischen Schräglaufverhalten von Kraftfahrzeugreifen bei beliebigen Felgenbewegungen. Fortschritt-Berichte VDI.: Verkehrstechnik/Fahrzeugtechnik. VDI-Verlag (1993). URL <https://books.google.de/books?id=JwpBmwEACAAJ>